

Coordinated logistics with a truck and a drone

John Gunnar Carlsson and Siyuan Song

Abstract

We determine the efficiency of a delivery system in which an unmanned aerial vehicle (UAV), or a fleet of UAVs, provides service to customers while making return trips to a truck that is itself moving. In other words, a UAV picks up a package from the truck (which continues on its route), and after delivering the package, the UAV returns to the truck to pick up the next package. Although the hardware for such systems already exists, it is not yet understood to what extent such an approach can actually provide a significantly improved quality of service. By combining a theoretical analysis in the Euclidean plane with real-time numerical simulations on a road network, we conclude that the improvement in efficiency due to introducing a UAV is proportional to the square root of the ratio of the speeds of the truck and the UAV.

1 Introduction

One of the most talked-about developments in transportation and logistics in recent years has been the potential use of unmanned aerial vehicles (UAVs), or “drones”, for transporting packages, food, medicine, and other goods. The most famous proof-of-concept of such a service is the “Amazon Prime Air” system, which was introduced in late 2013 and has since undergone several iterations [8]. Other similar systems include Google’s “Project Wing” [29], DHL’s “Parcelcopter” [9], and a joint effort between the Swiss Post, Swiss Worldcargo (the air freight division of Swiss International Air Lines), and the California-based startup Matternet [14]. As described in [25], there are many reasons to be optimistic about the role that UAVs can play in next-generation logistics systems:

[Demand for last-mile delivery] is likely to increase as e-commerce volumes grow.
... UAVs could provide major relief for inner cities, taking traffic off the roads and into the skies. So far, payloads are limited but a network of UAVs could nevertheless

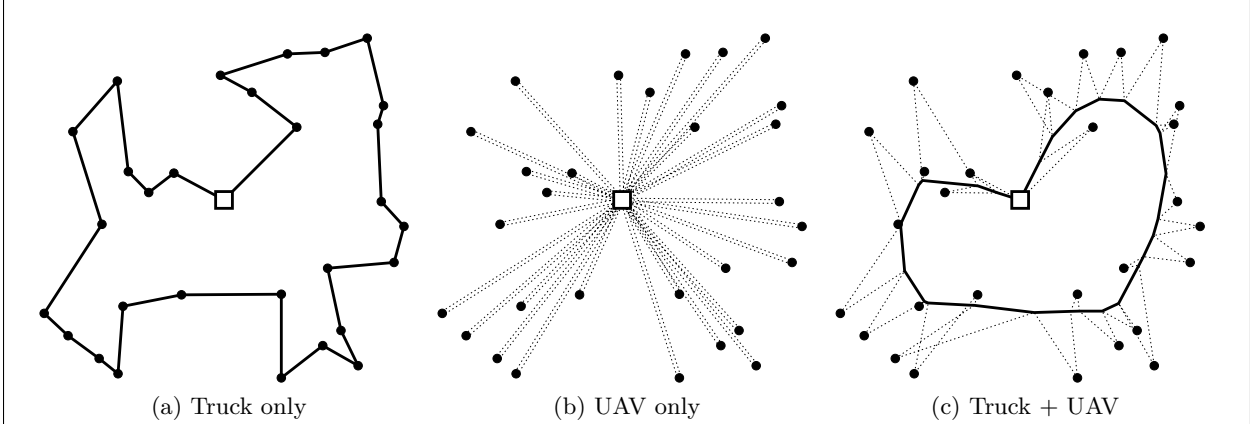


Figure 1: (a) shows a travelling salesman tour of a set of client destinations and a central depot, which corresponds to the optimal provision of service by a delivery scheme that uses only a truck. Similarly, (b) shows a collection of direct trips between the same set of points and the central depot, which corresponds to the optimal provision of service by a delivery scheme that uses only UAVs. Finally, (c) shows the solution to a problem in which we have a truck that follows a route that is much shorter than that of (a), as indicated by the thick tour, as well as a single UAV that alternates between visiting the client destinations and the truck, as indicated by the dashed lines. The routes shown correspond to the case where the UAV is about four times as fast as the truck; it is also worth mentioning that the optimal sequence of the client destinations is not necessarily the same as that induced by the TSP tour which is shown in (a), and indeed one can readily observe that there are several places where the two sequences differ.

support first and last-mile logistics networks. ... This urban first and last-mile use case is probably the most tangible and spectacular in the logistics industry.

UAVs are also already being used in many related industries including energy [38], agriculture and forestry [4], environmental protection [34], and emergency response [33].

From a transportation scientist's perspective, many of the benefits of a UAV-based delivery system are obvious: UAVs have a low per-mile cost, can operate without human intervention, and can travel at high speeds while being unaffected by road traffic. The shortcomings of such a system are equally apparent: UAVs have an extremely low carrying capacity and short travelling radius, both of which necessitate frequent returns to a central depot. Thus, as suggested in Figures 1a and 1b, a conventional truck delivery system benefits from an economy of scale and suffers from high per-mile costs, whereas a UAV delivery system benefits from low per-mile costs and lacks an economy of scale.

The purpose of this paper is to determine the efficiency of a hybrid approach in which a UAV (or a fleet of UAVs) provides service to customers while making return trips to a truck that is itself

moving, as illustrated in Figure 1c. In other words, a UAV picks up a package from the truck (which continues on its route), and after delivering the package, the UAV returns to the truck to pick up the next package. Although the hardware for such systems has already been constructed – one particular implementation is called the “HorseFly” and was developed jointly with AMP Electric Vehicles and the University of Cincinnati [43] – it is not yet understood to what extent such an approach can actually provide a significantly improved quality of service. Our goal is to describe precisely how much improvement can be realized in a mathematically sound way.

Obviously, the “horsefly” problem is extremely difficult to solve to optimality because it is a generalization of the travelling salesman problem (TSP) that requires the consideration of the locations where the truck and the UAV meet. Thus, we approach this problem from the *continuous approximation paradigm*, in which “detailed data are replaced by concise summaries, and numerical methods are replaced by analytic models” [15]; our goal is to reduce the problem to a small set of parameters, and then determine how these parameters affect the outcome of the problem. In a nutshell, our model assumes that customers are distributed according to a known probability density in the Euclidean plane. We primarily focus on the *time to completion* of all of the deliveries, and our results are also easily applicable to other cost functions such as the net energy expenditure over both vehicles.

The remainder of this paper is structured as follows: Section 2 defines our problem formally and also gives a pair of geometric results. Section 3 gives upper and lower bounds for the time to completion of a tour under the assumption that demand is continuously distributed in the Euclidean plane, and characterizes the amount of improvement that is realized by a hybrid system in terms of the speeds of the truck and the UAV. Finally, Section 4 describes two computational simulations that verify that our continuous approximation result is a valid one in practice; one simulation is conducted in the Euclidean plane, whereas the other uses real-time driving information on a road network using the Google Directions API [3].

1.1 Related work

The use of UAVs in logistics is a prospect that is very much in its infancy, and as such, there is little research on the economics of such systems. The recent papers [5, 22, 35] all describe mixed integer programming formulations and heuristic algorithms for solving several optimization problems in

which a truck and a UAV perform service in tandem. Even more recently, [42] describes “worst-case” configurations of input points that minimize the benefit that a UAV can offer in assisting a truck; their analysis further enables one to make “best-case” predictions as well, by establishing that the improvement offered by adding a UAV (or multiple UAVs) cannot exceed a certain value. Instead of examining solutions to specific problem instances or examining worst- or best-case scenarios, our paper – by comparison – is concerned with the long-term behavior when many customers are serviced in a region according to a population density (this is the principle of the continuous approximation paradigm for transportation, which we discuss later in this section). The most concrete discussion of the economic desirability thus far can be found in [16], which analyzes per-mile costs based on the estimated energy consumption of UAVs and describes several feasibility issues in implementation; the author concludes that “From a cost perspective, the numbers do not look unreasonable”. Within the operations research community, extensive research has been conducted on the use of UAVs for military applications; for example, [18] uses robust optimization to plan reconnaissance missions subject to uncertainty in fuel usage between locations and weather conditions and [31] uses scenario-based optimization to decide the number of UAVs to deploy; once deployed, more information about the environment is learned, at which point the route must be determined.

Our problem can essentially be thought of as an intermodal instance of the *Vehicle Routing Problem* (VRP) [20, 41]. Because we seek to optimally coordinate two classes of vehicles that have diametrically opposing strengths and weaknesses, our problem is particularly related to instances of VRP in which vehicle heterogeneity plays an important role, such as [21]. A closely related problem to ours is described in [32], which gives an integer programming formulation and a heuristic algorithm for solving a routing problem in which a truck can carry a fleet of “foot couriers” on a single- or multi-route assignment, and the goal is to coordinate resources between the truck and the couriers effectively.

One of the basic phenomena that is of interest to us is the trade-off between efficiency in transportation along a backbone network (in this case, the route of the truck) versus direct trips between locations (in this case, the direct trips taken by UAVs); this is arguably one of the fundamental dichotomies in transportation and logistics [12, 13]. In this sense, our problem of interest is philosophically similar to [11], which asks whether small local retail stores are preferable to “big-box”

retailers, with [44], which estimates the changes in net CO₂ emissions that result by introducing grocery delivery services, and with [45], which computes the optimal layout of a set of facility locations that are themselves connected with a backbone network.

This paper is concerned with a *continuous approximation* model for a transportation problem, and is therefore philosophically similar to (for example) [10], which analytically determines trade-offs between transportation and inventory costs, [27], which shows how to route emergency relief vehicles to beneficiaries in a time-sensitive manner, and [28], which describes a simple geometric model for determining the optimal mixture of a fleet of vehicles that perform distribution. The basic premise of the continuous approximation paradigm is that one replaces combinatorial quantities that are difficult to compute with simpler mathematical formulas, which (under certain conditions) provide accurate estimations of the desired quantity (and indeed, we will verify in Section 4 that our theoretical analysis holds under realistic modelling assumptions). Such approximations exist for many combinatorial problems, such as the travelling salesman problem [7, 19], facility location [23, 26, 36], and any *subadditive Euclidean functional* such as a minimum spanning tree, Steiner tree, or matching [37, 39, 40].

1.2 Notational conventions

Our notational conventions are as follows: we assume that there are n customer locations in the Euclidean plane to be visited with a truck and a UAV whose speeds are ϕ_0 and ϕ_1 respectively, with $\phi_0 < \phi_1$. These customers are assumed to follow an absolutely continuous probability distribution f , which is defined on a compact planar region \mathcal{R} . We use \mathcal{L} to denote a loop in \mathcal{R} (representing the truck's tour), we use $\text{Loop}(\mathcal{R})$ to denote the set of *all* loops \mathcal{L} in \mathcal{R} whose length is well-defined, and we let $d(x, \mathcal{L})$ denote the distance between point x to loop \mathcal{L} ; that is,

$$d(x, \mathcal{L}) = \min_{x' \in \mathcal{L}} \|x - x'\|,$$

where $\|\cdot\|$ is the usual Euclidean distance. The set of permutations of $\{1, \dots, n\}$ will be written as S_n , with a particular permutation written as $\sigma \in S_n$; because these permutations always correspond to a tour that our truck takes, we will adopt the convention that $\sigma(n+1) = \sigma(1)$ for brevity. The

(closed) ϵ -neighborhood of a (compact) set \mathcal{S} in the plane will be written as $N_\epsilon(\mathcal{S})$, which is to say,

$$N_\epsilon(\mathcal{S}) = \{x \in \mathbb{R}^2 : \min_{x' \in \mathcal{S}} \|x - x'\| \leq \epsilon\}.$$

We say that a function $g(x)$ satisfies $g(x) \sim h(x)$ as $x \rightarrow \infty$ if $\lim_{x \rightarrow \infty} g(x)/h(x) = 1$. Finally, we use the expression $\mathbb{1}_{x \in \mathcal{S}}$ to denote the indicator function for membership in set \mathcal{S} .

2 Preliminaries

We begin by formally defining the *horsefly routing problem* in which we coordinate a truck and a single UAV:

Definition 1 (Horsefly routing with one truck and one UAV). Let p_1, \dots, p_n be a collection of points in the plane and let $\phi_0, \phi_1 > 0$ denote the speeds of a truck and a UAV respectively, with $\phi_0 < \phi_1$. The optimal *horsefly tour* of p_1, \dots, p_n is the solution to the optimization problem

$$\underset{x_1, \dots, x_n, \sigma \in S_n}{\text{minimize}} \sum_{i=1}^n \max \left\{ \frac{1}{\phi_0} \|x_{\sigma(i)} - x_{\sigma(i+1)}\|, \frac{1}{\phi_1} (\|x_{\sigma(i)} - p_{\sigma(i)}\| + \|p_{\sigma(i)} - x_{\sigma(i+1)}\|) \right\} \quad (1)$$

where $S_n \ni \sigma$ is the set of all permutations of the set $\{1, \dots, n\}$, with the added convention that $\sigma(n+1) = \sigma(1)$ for notational convenience.

Figure 2 shows an example of a solution to the above problem. Each variable x_i corresponds to the “launch site” at which the truck releases the UAV to visit customer point p_i ; the first term in the $\max\{\cdot, \cdot\}$ expression simply corresponds to the amount of time needed for the truck to move from one launch site to the next, whereas the second term corresponds to the amount of time needed for the UAV to leave its launch site, arrive at its customer point, and return to rendezvous with the truck at the next launch site. The generalization of (1) that arises when one has *multiple* UAVs is also important and will be discussed in Section 3.3. It is worth noting that, if one fixes the permutation σ , the remaining optimization problem over variables x_i is convex.

The following classical theorem, originally stated in [7] and further developed in [39, 40], relates the length of a TSP tour of a sequence of points with the distribution from which they were sampled:

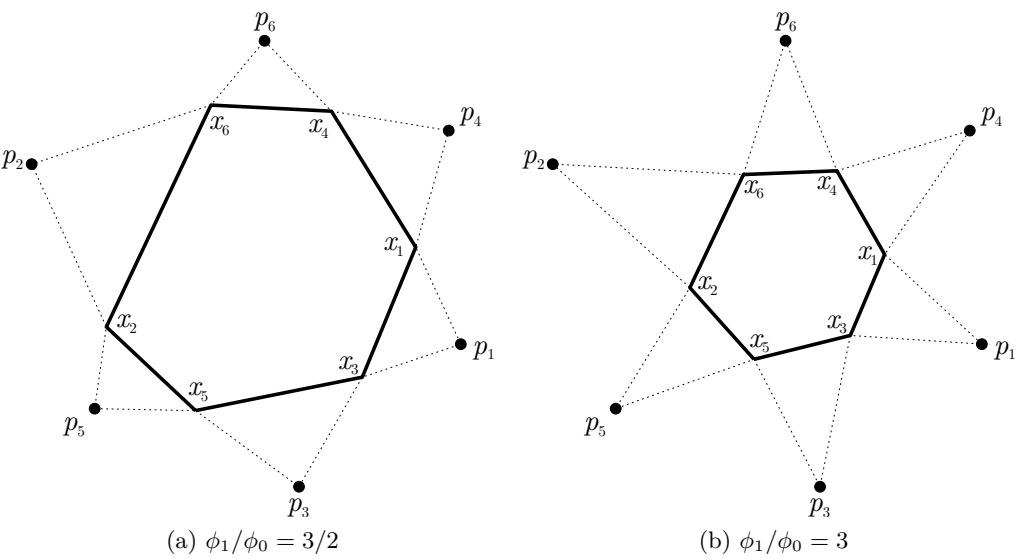


Figure 2: Solutions to an instance of the horsefly routing problem, with points p_1, \dots, p_6 as shown and with $\phi_1/\phi_0 = 3/2$ and $\phi_1/\phi_0 = 3$ respectively. Defining x_1 arbitrarily as a starting point, we have $\sigma = \{1, 3, 5, 2, 6, 4\}$ in both routes. The fact that $\phi_1/\phi_0 = 3/2$ in (a) is reflected by the observation that each pair of dashed line segments to and from a customer point $p_{\sigma(i)}$ (corresponding to a UAV's trip that starts with the truck, visits the customer, and returns to the truck) has length equal to $3/2$ that of the thickened line segment from $x_{\sigma(i)}$ to $x_{\sigma(i+1)}$. Similarly, in (b), each pair of dashed line segments has length equal to 3 times that of the corresponding thickened line segment.

Theorem 2 (BHH Theorem). *Suppose that $X = \{X_1, X_2, \dots\}$ is a sequence of random points i.i.d. according to an absolutely continuous probability density function f defined on a compact planar region \mathcal{R} . Then with probability one, the length $\text{TSP}(X)$ of the optimal travelling salesman tour through X satisfies*

$$\lim_{N \rightarrow \infty} \frac{\text{TSP}(X)}{\sqrt{N}} = \beta \iint_{\mathcal{R}} \sqrt{f(x)} \, dx$$

where β is a constant.

It is additionally known that $0.6250 \leq \beta \leq 0.9204$ and estimated that $\beta \approx 0.7124$; see [6, 7].

The following geometric result will be helpful to us later in relating the workload of the truck and the workload of the UAV; given a loop \mathcal{L} (which represents the tour taken by the truck), it is useful to know how much area is within a given distance ϵ of \mathcal{L} :

Lemma 3. *Let \mathcal{L} be a loop in the plane with length ℓ and let $\epsilon > 0$. The area of an ϵ -neighborhood of \mathcal{L} is at most*

$$\text{Area}(N_\epsilon(\mathcal{L})) \leq \begin{cases} 2\epsilon\ell & \text{if } \epsilon \leq \frac{\ell}{2\pi} \\ \pi\epsilon^2 + \epsilon\ell + \frac{\ell^2}{4\pi} & \text{otherwise,} \end{cases}$$

which is tight when \mathcal{L} is a circle, whereby $N_\epsilon(\mathcal{L})$ is either an annulus (if $\epsilon \leq \ell/(2\pi)$) or a disk (if $\epsilon > \ell/(2\pi)$).

Proof. Assume without loss of generality that \mathcal{L} forms the boundary of a convex region and that \mathcal{L} is piecewise linear, i.e. polygonal (see the appendix for justifications of both of these assumptions). The ϵ -neighborhood of \mathcal{L} has an “inner” portion R_{in} and an “outer” portion R_{out} as shown in Figure 3a, and we can also see from Figure 3a that the area of the “outer” portion R_{out} is always exactly $\pi\epsilon^2 + \epsilon\ell$. It is also obvious that the outer perimeter of R_{out} is exactly $\ell + 2\pi\epsilon$. The area of the “inner” portion R_{in} is a little more complicated to bound; first, for any $\epsilon' \leq \epsilon$, we let $\mathcal{L}_{\epsilon'}$ denote the closed curve inside \mathcal{L} consisting of points that are *exactly* ϵ' away from their nearest point in \mathcal{L} (thus, our original \mathcal{L} would simply be written as \mathcal{L}_0 under this notation). It is of course possible that $\mathcal{L}_{\epsilon'} = \emptyset$ for sufficiently large ϵ' . Since R_{in} is simply the union of all curves $\mathcal{L}_{\epsilon'}$ over $\epsilon' \in [0, \epsilon]$, the *coarea formula* [30] says that the area of R_{in} is obtained by simply integrating the length of $\mathcal{L}_{\epsilon'}$ from $\epsilon' = 0$ to $\epsilon' = \epsilon$:

$$\text{Area}(R_{\text{in}}) = \int_0^\epsilon \text{length}(\mathcal{L}_{\epsilon'}) \, d\epsilon'.$$

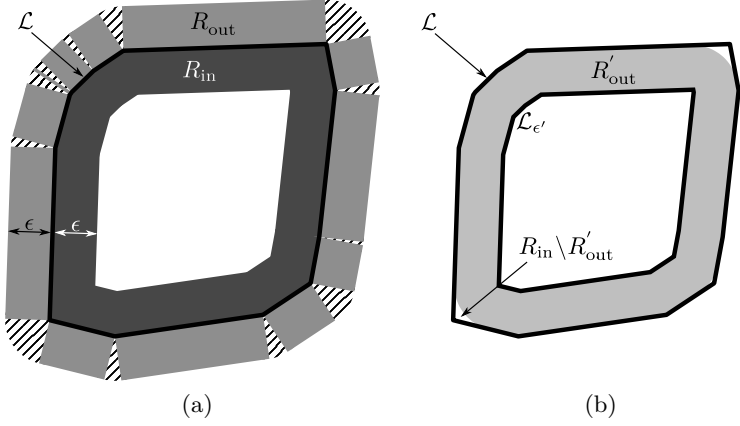


Figure 3: (a) shows the neighborhoods R_{in} and R_{out} ; note that R_{out} is the union of the shaded rectangles and the hatched circular sectors, and therefore $\text{Area}(R_{\text{out}}) = \pi\epsilon^2 + \epsilon\ell$ and $\text{perimeter}(R_{\text{out}}) = \ell + 2\pi\epsilon$. (b) shows an inner loop $\mathcal{L}_{\epsilon'}$ and illustrates that $R'_{\text{out}} \subseteq R_{\text{in}}$ for all ϵ' (which characterize R'_{out}).

Let R'_{out} denote the “outer” portion of the ϵ' -neighborhood of $\mathcal{L}_{\epsilon'}$, as shown in Figure 3b. We then have $R'_{\text{out}} \subseteq R_{\text{in}}$, which by convexity implies that the outer perimeter of R'_{out} is less than or equal to the length of \mathcal{L} , i.e. ℓ . However, by the same reasoning as our calculation of the outer perimeter of R_{out} , we also see that the outer perimeter of R'_{out} is exactly $\text{length}(\mathcal{L}_{\epsilon'}) + 2\pi\epsilon'$, and therefore

$$\begin{aligned}\ell &= \text{length}(\mathcal{L}) \geq \text{perimeter}(R'_{\text{out}}) = \text{length}(\mathcal{L}_{\epsilon'}) + 2\pi\epsilon' \\ \implies \text{length}(\mathcal{L}_{\epsilon'}) &\leq \ell - 2\pi\epsilon'\end{aligned}$$

provided that $\mathcal{L}_{\epsilon'}$ exists, i.e. that $\text{length}(\mathcal{L}_{\epsilon'}) > 0$. Thus, we see that

$$\text{Area}(R_{\text{in}}) = \int_0^\epsilon \text{length}(\mathcal{L}_{\epsilon'}) d\epsilon' \leq \int_0^\epsilon \max\{\ell - 2\pi\epsilon', 0\} d\epsilon' = \begin{cases} \epsilon\ell - \pi\epsilon^2 & \text{if } \epsilon \leq \frac{\ell}{2\pi} \\ \frac{\ell^2}{4\pi} & \text{otherwise} \end{cases}$$

from which the desired result follows, since $\text{Area}(N_\epsilon(\mathcal{L})) = \text{Area}(R_{\text{in}}) + \text{Area}(R_{\text{out}})$. \square

3 Asymptotic analysis of the horsefly routing problem

This section derives upper and lower bounds for a continuous approximation of problem (1), under the assumption that the customers are distributed according to a known absolutely continuous

probability distribution f . Not surprisingly, it is useful to describe the average distance between a customer sampled from f and a loop \mathcal{L} :

Theorem 4. *Let \mathcal{R} be a compact planar region and let f be an absolutely continuous probability density function defined on \mathcal{R} . Let $\text{OPT}(\ell)$ denote the optimal objective value to the problem*

$$\begin{aligned} \underset{\mathcal{L} \in \text{Loop}(\mathcal{R})}{\text{minimize}} \quad & \iint_{\mathcal{R}} f(x) d(x, \mathcal{L}) dx \quad \text{s.t.} \\ & \text{length}(\mathcal{L}) = \ell, \end{aligned} \tag{2}$$

where the optimization variable \mathcal{L} is taken over the set of all loops in \mathcal{R} whose length is well-defined.

Then

$$\text{OPT}(\ell) \sim \frac{1}{4\ell} \left(\iint_{\mathcal{R}} \sqrt{f(x)} dx \right)^2$$

as $\ell \rightarrow \infty$.

Figure 4d shows an example of an optimal solution to this problem. In order to prove Theorem 4, it is easiest first to consider the special case where f is a uniform distribution:

Lemma 5. *Let \mathcal{L} be a loop in a compact region \mathcal{R} with area A . Then $\iint_{\mathcal{R}} d(x, \mathcal{L}) dx$ satisfies*

$$\iint_{\mathcal{R}} d(x, \mathcal{L}) dx \geq \begin{cases} \frac{2A^{3/2}}{3\sqrt{\pi}} - \frac{A\ell}{2\pi} + \frac{\ell^3}{12\pi^2} & \text{if } \ell \leq \sqrt{A\pi} \\ \frac{A^2}{4\ell} & \text{otherwise.} \end{cases} \tag{3}$$

Proof. We can assume without loss of generality that $A = 1$ because, if we apply the transformation $A \mapsto cA$ and $\ell \mapsto \sqrt{c}\ell$ for any $c > 0$, then the right-hand side of the above is simply scaled by $c^{3/2}$. Thus, the quantity of interest $\iint_{\mathcal{R}} d(x, \mathcal{L}) dx$ is simply equal to the expected distance between a point X uniformly sampled in \mathcal{R} and \mathcal{L} , i.e. $\mathbf{E}d(X, \mathcal{L})$. Recall that for any non-negative random variable Z on the real line, we have

$$\mathbf{E}(Z) = \int_0^\infty 1 - F(z) dz,$$

where F is the cumulative distribution function of Z (this is a simple consequence of integration by parts [24]). If we set $Z = d(X, \mathcal{L})$, where X is uniformly sampled in \mathcal{L} , then Lemma 3 tells us

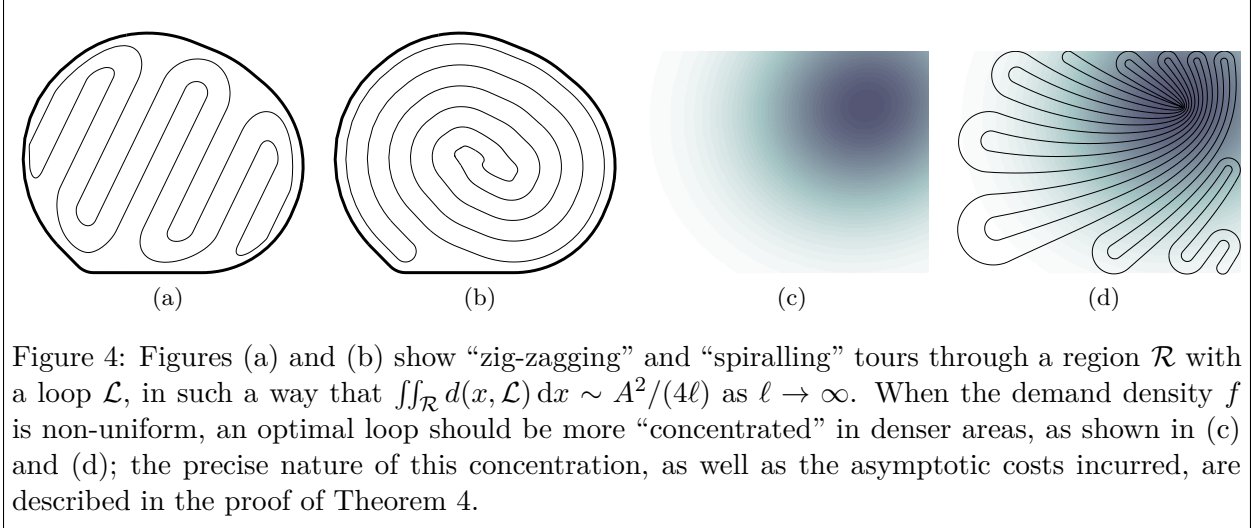


Figure 4: Figures (a) and (b) show “zig-zagging” and “spiralling” tours through a region \mathcal{R} with a loop \mathcal{L} , in such a way that $\iint_{\mathcal{R}} d(x, \mathcal{L}) dx \sim A^2/(4\ell)$ as $\ell \rightarrow \infty$. When the demand density f is non-uniform, an optimal loop should be more “concentrated” in denser areas, as shown in (c) and (d); the precise nature of this concentration, as well as the asymptotic costs incurred, are described in the proof of Theorem 4.

that

$$F(z) = \text{Area}(N_z(\mathcal{L}) \cap \mathcal{R}) \leq \text{Area}(N_z(\mathcal{L})) \leq \begin{cases} 2z\ell & \text{if } z \leq \frac{\ell}{2\pi} \\ \pi z^2 + z\ell + \frac{\ell^2}{4\pi} & \text{otherwise.} \end{cases}$$

Suppose that $\ell > \sqrt{\pi}$ as in the second case of the desired inequality. We then have

$$\iint_{\mathcal{R}} d(x, \mathcal{L}) dx = \mathbf{E} d(X, \mathcal{L}) = \int_0^\infty 1 - F(z) dz \geq \int_0^{\frac{1}{2\ell}} 1 - F(z) dz \geq \int_0^{\frac{1}{2\ell}} 1 - 2z\ell dz = \frac{1}{4\ell}.$$

On the other hand, if $\ell \leq \sqrt{\pi}$ as in the first case of the desired inequality, we have $\ell/(2\pi) \leq 1/\sqrt{\pi} - \ell/(2\pi)$, whence

$$\begin{aligned} \iint_{\mathcal{R}} d(x, \mathcal{L}) dx &= \int_0^\infty 1 - F(z) dz \geq \int_0^{\frac{\ell}{2\pi}} 1 - F(z) dz + \int_{\frac{\ell}{2\pi}}^{\frac{1}{\sqrt{\pi}} - \frac{\ell}{2\pi}} 1 - F(z) dz \\ &\geq \int_0^{\frac{\ell}{2\pi}} 1 - 2z\ell dz + \int_{\frac{\ell}{2\pi}}^{\frac{1}{\sqrt{\pi}} - \frac{\ell}{2\pi}} 1 - (\pi z^2 + z\ell + \frac{\ell^2}{4\pi}) dz = \frac{2}{3\sqrt{\pi}} - \frac{\ell}{2\pi} + \frac{\ell^3}{12\pi^2} \end{aligned}$$

which completes the proof. \square

Remark 6. As in Lemma 3, the lower bound (3) is tight when \mathcal{L} is a circle and \mathcal{R} is either an annulus or a disk. When \mathcal{R} is an arbitrary region, we can construct a family of loops \mathcal{L} with length ℓ that satisfy $\iint_{\mathcal{R}} d(x, \mathcal{L}) dx \sim A^2/(4\ell)$ as $\ell \rightarrow \infty$ by “zig-zagging” or “spiralling” through \mathcal{R} , as shown in Figures 4a and 4b. In the non-uniform case, the optimal solution to (2) is to zig-zag or spiral in a way that is consistent with the demand density f , as can be seen in Figure 4d.

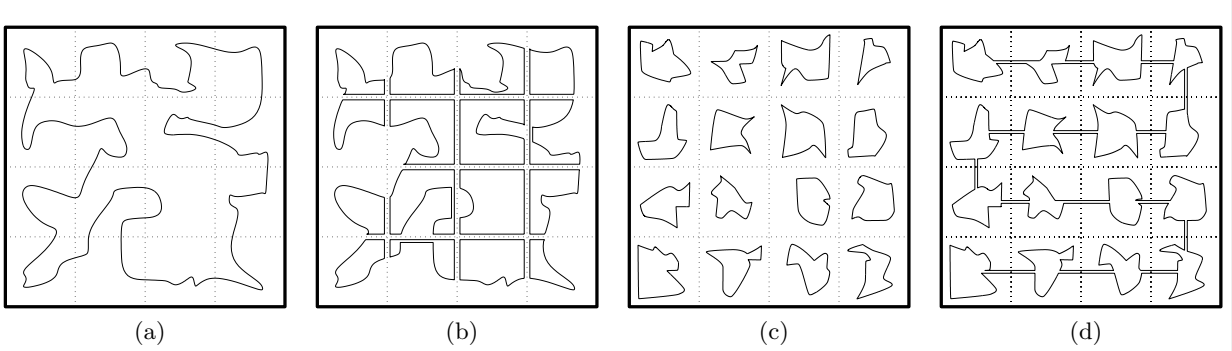


Figure 5: In the above diagrams, we have $N = 16$ square patches \mathcal{P}_i . Figures (a) and (b) show that one can always decompose a single loop into multiple loops in a way that depends only on the shapes of the patches. Figures (c) and (d) show that one can always join a collection of loops into a single loop in a way that also depends only on the shapes of the patches.

Theorem 4 is now straightforward:

Proof of Theorem 4. It will suffice to show that, given any threshold $\epsilon > 0$ together with \mathcal{R} and f , it is always possible to select a length $\bar{\ell}$ such that the optimal objective value to problem (2), i.e. $\text{OPT}(\ell)$, satisfies

$$\frac{1-\epsilon}{4\ell} \left(\iint_{\mathcal{R}} \sqrt{f(x)} dx \right)^2 \leq \text{OPT}(\ell) \leq \frac{1+\epsilon}{4\ell} \left(\iint_{\mathcal{R}} \sqrt{f(x)} dx \right)^2$$

for all $\ell \geq \bar{\ell}$. Because f is absolutely continuous, it is possible to approximate f arbitrarily well with a step function $\bar{f} = \sum_{i=1}^N \bar{f}_i$, where each component \bar{f}_i is a constant function on a patch $\mathcal{P}_i \subset \mathcal{R}$. That is, $\bar{f}_i(x) = a_i \mathbb{1}_{x \in \mathcal{P}_i}$ for positive scalars a_i , where $\mathbb{1}_{x \in \mathcal{P}_i}$ is the indicator function for membership in \mathcal{P}_i . Given any loop \mathcal{L} in \mathcal{R} , it is always possible to create a *collection* of loops $\mathcal{L}_i \subset \mathcal{P}_i$ such that $\mathcal{L} \subseteq \bigcup_i \mathcal{L}_i$ and $\sum_i \text{length}(\mathcal{L}_i) \leq \text{length}(\mathcal{L}) + c_1$, where c_1 is a constant that depends only on the patches \mathcal{P}_i (for example, c_1 is bounded above by the sum of the perimeters of the \mathcal{P}_i 's); this is illustrated in Figures 5a and 5b. Similarly, given any collection of loops $\mathcal{L}_i \subset \mathcal{P}_i$, it is always possible to create a *single loop* \mathcal{L} such that $\bigcup_i \mathcal{L}_i \subseteq \mathcal{L}$ and such that $\text{length}(\mathcal{L}) \leq \sum_i \text{length}(\mathcal{L}_i) + c_2$, where c_2 again depends only on the patches; this is illustrated in Figures 5c and 5d. These observations are useful to us because we are interested in the limiting behavior of (2) as $\ell \rightarrow \infty$, and we see that c_1 and c_2 are independent of ℓ .

Given a desired threshold $\epsilon > 0$, choose $\delta > 0$ so that $(1 - \epsilon) \leq (1 - \delta)^2 < (1 + \delta)^2 \leq (1 + \epsilon)$

and let \bar{f} be a sufficiently fine approximation that $(1 - \delta)\bar{f}(x) \leq f(x) \leq (1 + \delta)\bar{f}(x)$ for all $x \in \mathcal{R}$.

For reasons that will be clear later, we will also require that \bar{f} be chosen so that

$$1 - \delta \leq \frac{\iint_{\mathcal{R}} \sqrt{f(x)} dx}{\iint_{\mathcal{R}} \sqrt{\bar{f}(x)} dx} \leq 1 + \delta.$$

By our previous observations, $\text{OPT}(\ell)$ is bounded above by the optimal solution to

$$\begin{aligned} & \underset{\mathcal{L}_1, \dots, \mathcal{L}_N}{\text{minimize}} (1 + \delta) \sum_{i=1}^N \iint_{\mathcal{P}_i} \bar{f}_i(x) d(x, \mathcal{L}_i) dx \\ & \quad \sum_{i=1}^N \text{length}(\mathcal{L}_i) = \ell - c, \end{aligned} \tag{4}$$

where each \mathcal{L}_i is a loop in patch \mathcal{P}_i . Consider the problem of selecting a single optimal loop $\mathcal{L}_i \subset \mathcal{P}_i$, under the assumption that $\text{length}(\mathcal{L}_i) = \ell_i$ is known; this is written as

$$\begin{aligned} & \underset{\mathcal{L}_i \in \text{Loop}(\mathcal{P}_i)}{\text{minimize}} \iint_{\mathcal{P}_i} \bar{f}_i d(x, \mathcal{L}_i) dx \quad s.t. \\ & \quad \text{length}(\mathcal{L}_i) = \ell_i, \end{aligned} \tag{5}$$

and since $\bar{f}_i(x) = a_i$ on \mathcal{P}_i , we therefore can apply Lemma 5 and Remark 6, which say that, for sufficiently large ℓ_i , the optimal objective value of (5) is asymptotically equal to $a_i \text{Area}(\mathcal{P}_i)^2/(4\ell_i)$; moreover, this is realizable by “zig-zagging” or “spiralling” in \mathcal{P}_i as in Figure 4. Thus, we see that as $\ell \rightarrow \infty$, problem (4) is asymptotically equivalent to the problem

$$\begin{aligned} & \underset{\ell_1, \dots, \ell_N}{\text{minimize}} (1 + \delta) \sum_{i=1}^N a_i \cdot \frac{\text{Area}(\mathcal{P}_i)^2}{4\ell_i} \quad s.t. \\ & \quad \sum_{i=1}^N \ell_i = \ell - c \\ & \quad \ell_i \geq 0 \end{aligned} \tag{6}$$

as $\ell \rightarrow \infty$. The optimal solution to (6) is to set

$$\ell_i^* = \frac{\sqrt{a_i} \text{Area}(\mathcal{P}_i)}{\sum_{i=1}^N \sqrt{a_i} \text{Area}(\mathcal{P}_i)} \cdot (\ell - c)$$

for each i , which gives an objective value of

$$\begin{aligned}
(1 + \delta) \sum_{i=1}^N a_i \cdot \frac{\text{Area}(\mathcal{P}_i)^2}{4\ell_i^*} &= \frac{1 + \delta}{4(\ell - c)} \left(\sum_{j=1}^N \sqrt{a_j} \text{Area}(\mathcal{P}_j) \right)^2 = \frac{1 + \delta}{4(\ell - c)} \left(\iint_{\mathcal{R}} \sqrt{\bar{f}(x)} dx \right)^2 \\
&\leq \frac{(1 + \delta)^2}{4(\ell - c)} \left(\iint_{\mathcal{R}} \sqrt{f(x)} dx \right)^2 \\
\implies \text{OPT}(\ell) &\leq \frac{1 + \epsilon}{4(\ell - c)} \left(\iint_{\mathcal{R}} \sqrt{f(x)} dx \right)^2.
\end{aligned}$$

We can also derive a lower bound of (2) using nearly identical reasoning, because $\text{OPT}(\ell)$ is bounded *below* by the optimal solution to

$$\begin{aligned}
\underset{\mathcal{L}_1, \dots, \mathcal{L}_N}{\text{minimize}} (1 - \delta) \sum_{i=1}^N \iint_{\mathcal{P}_i} \bar{f}_i(x) d(x, \mathcal{L}_i) dx \\
\sum_{i=1}^N \text{length}(\mathcal{L}_i) = \ell + c
\end{aligned}$$

and an entirely analogous argument shows that

$$\text{OPT}(\ell) \geq \frac{1 - \epsilon}{4(\ell + c)} \left(\iint_{\mathcal{R}} \sqrt{f(x)} dx \right)^2$$

for sufficiently large ℓ , which completes the proof. \square

Remark 7. It is not surprising that the expression $\iint_{\mathcal{R}} \sqrt{f(x)} dx$ should appear because of its connection to the length of the TSP tour as established in Theorem 2. Indeed, our proof strategy for Theorem 4 is similar to Section 2.4 of [40].

Remark 8. Within patch \mathcal{P}_i , if we let loop \mathcal{L}_i be a “zig-zag” or “spiral” with length ℓ_i as in Figure 4, then standard arguments show that the distance $d(X, \mathcal{L}_i)$ to a random point X sampled uniformly in \mathcal{P}_i satisfies $\ell_i \cdot d(X, \mathcal{L}_i) \rightarrow \mathcal{U}[0, \text{Area}(\mathcal{P}_i)/2]$ almost surely as $\ell_i \rightarrow \infty$, where $\mathcal{U}[\cdot, \cdot]$ denotes a uniformly distributed random variable. Stated informally, this means that $d(X, \mathcal{L}_i)$ is approximately uniformly distributed between 0 and $\text{Area}(\mathcal{P}_i)/(2\ell_i)$. By using the expression for the optimal ℓ_i^* together with the fact that \bar{f} is an approximation of the absolutely continuous density f , we conclude that the distance between an optimal loop \mathcal{L} and a point X sampled from f , conditioned on the fact that X is near a fixed point x_0 , is (approximately) uniformly distributed

between 0 and

$$\frac{\int f(x) dx}{2\ell} \cdot \frac{1}{\sqrt{f(x_0)}}.$$

We will make use of this fact in Section 3.3, which describes how to analyze a horsefly problem with more than one UAV.

3.1 A lower bound

It is fairly straightforward to derive a lower bound of problem (1) that is more amenable to asymptotic analysis:

Claim 9. The optimal objective value to the problem

$$\underset{x_1, \dots, x_n, \sigma \in S_n}{\text{minimize}} \max \left\{ \frac{1}{\phi_0} \sum_{i=1}^n \|x_{\sigma(i)} - x_{\sigma(i+1)}\|, \frac{2}{\phi_1} \sum_{i=1}^n \|x_i - p_i\| \right\} \quad (7)$$

is a lower bound of problem (1).

Proof. This is sketched in Figure 6. Let x_1, \dots, x_n and σ be any input to problem (1) and let \mathcal{L} denote the loop that is obtained by visiting the points x_i in the order determined by σ (in other words, \mathcal{L} is the truck's route). For each point p_i , let x'_i be the point on \mathcal{L} that is closest to point p_i . We then certainly have $\|x - p_i\| \geq \|x'_i - p_i\|$ for all $x \in \mathcal{L}$ by definition, and therefore the objective value of (1) satisfies

$$\begin{aligned} & \sum_{i=1}^n \max \left\{ \frac{1}{\phi_0} \|x_{\sigma(i)} - x_{\sigma(i+1)}\|, \frac{1}{\phi_1} (\|x_{\sigma(i)} - p_{\sigma(i)}\| + \|p_{\sigma(i)} - x_{\sigma(i+1)}\|) \right\} \\ & \geq \max \left\{ \sum_{i=1}^n \frac{1}{\phi_0} \|x_{\sigma(i)} - x_{\sigma(i+1)}\|, \frac{1}{\phi_1} \sum_{i=1}^n (\|x_{\sigma(i)} - p_{\sigma(i)}\| + \|p_{\sigma(i)} - x_{\sigma(i+1)}\|) \right\} \\ & \geq \max \left\{ \sum_{i=1}^n \frac{1}{\phi_0} \|x_{\sigma(i)} - x_{\sigma(i+1)}\|, \frac{2}{\phi_1} \sum_{i=1}^n \|x'_i - p_i\| \right\} \\ & \geq \max \left\{ \sum_{i=1}^n \frac{1}{\phi_0} \|x'_{\sigma'(i)} - x'_{\sigma'(i+1)}\|, \frac{2}{\phi_1} \sum_{i=1}^n \|x'_i - p_i\| \right\} \end{aligned}$$

where σ' is the optimal permutation corresponding to the optimal tour of the points x'_i . We therefore see that, for any input to (1), we can construct an input to (7) whose objective value is at most equal to that of (1), which completes the proof. \square

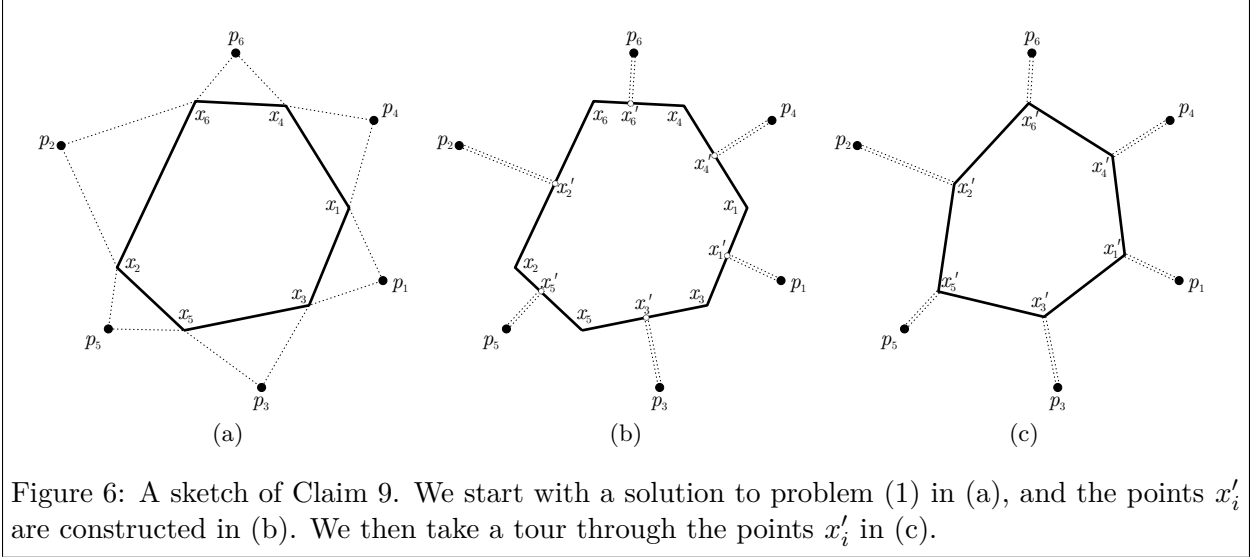


Figure 6: A sketch of Claim 9. We start with a solution to problem (1) in (a), and the points x'_i are constructed in (b). We then take a tour through the points x'_i in (c).

Both problem (1) and the lower bound (7) are parametrized in terms of the “launch sites” x_i because it is obvious that the truck should always move in a straight line from one launch site to the next (there is nothing to be gained by travelling on a curved path). It is also possible to express problem (7) as an infinite-dimensional optimization problem whose variable space is $\text{Loop}(\mathcal{R})$, the space of all *rectifiable loops* \mathcal{L} in \mathcal{R} , that is, all paths in \mathcal{R} whose start and end points are the same and whose length is well-defined. The equivalent problem of (7) would then be written as

$$\underset{\mathcal{L} \in \text{Loop}(\mathcal{R})}{\text{minimize}} \max \left\{ \frac{1}{\phi_0} \text{length}(\mathcal{L}), \frac{2}{\phi_1} \sum_{i=1}^n d(p_i, \mathcal{L}) \right\}, \quad (8)$$

where $d(p_i, \mathcal{L}) = \min_{x \in \mathcal{L}} \|p_i - x\|$ is the distance between p_i and its closest point in \mathcal{L} .

We now assume that customer demand points p_i are independent samples from an absolutely continuous probability density function f that is defined on \mathcal{R} . The summation in problem (8) then becomes an integral over \mathcal{R} , so that the continuous approximation to (8) takes the form

$$\underset{\mathcal{L} \in \text{Loop}(\mathcal{R})}{\text{minimize}} \max \left\{ \frac{1}{\phi_0} \text{length}(\mathcal{L}), \frac{2n}{\phi_1} \iint_{\mathcal{R}} f(x) d(x, \mathcal{L}) dx \right\}. \quad (9)$$

The optimal trade-off between the two components above is characterized as follows:

Theorem 10. *For fixed \mathcal{R} , f , ϕ_0 , and ϕ_1 , the optimal objective value $\text{OPT}(n)$ to problem (9)*

satisfies

$$\text{OPT}(n) \sim \sqrt{\frac{n}{2\phi_0\phi_1}} \cdot \iint_{\mathcal{R}} \sqrt{f(x)} \, dx$$

as $n \rightarrow \infty$.

Proof. It is obvious that, as $n \rightarrow \infty$, the optimal solution to (9) must have $\text{length}(\mathcal{L}) \rightarrow \infty$ as well.

By Theorem 4, we see that for optimal \mathcal{L} whose length ℓ is sufficiently large, we have

$$\frac{2n}{\phi_1} \iint_{\mathcal{R}} f(x) d(x, \mathcal{L}) \, dx \sim \frac{n}{2\phi_1\ell} \left(\iint_{\mathcal{R}} \sqrt{f(x)} \, dx \right)^2,$$

and therefore $\text{OPT}(n)$ is asymptotically equivalent to the problem

$$\underset{\ell \geq 0}{\text{minimize}} \max \left\{ \frac{\ell}{\phi_0}, \frac{n}{2\phi_1\ell} \left(\iint_{\mathcal{R}} \sqrt{f(x)} \, dx \right)^2 \right\}.$$

This is obviously solved by setting $\ell^* = \sqrt{\frac{\phi_0 n}{2\phi_1}} \cdot \iint_{\mathcal{R}} \sqrt{f(x)} \, dx$, which gives an objective value of $\sqrt{\frac{n}{2\phi_0\phi_1}} \cdot \iint_{\mathcal{R}} \sqrt{f(x)} \, dx$ as desired. \square

3.2 An upper bound

It is similarly easy to derive an upper bound of problem (1) that is also amenable to asymptotic analysis:

Claim 11. The optimal objective value to the problem

$$\underset{x_1, \dots, x_n, \sigma \in S_n}{\text{minimize}} \frac{1}{\phi_0} \sum_{i=1}^n \|x_{\sigma(i)} - x_{\sigma(i+1)}\| + \frac{2}{\phi_1} \sum_{i=1}^n \|x_i - p_i\| \quad (10)$$

is an upper bound of problem (1):

Proof. Problem (10) is nothing more than the total time required to complete a horsefly route when one is subject to an additional constraint that the truck must remain stationary whenever the drone is away from the vehicle (in other words, it is the sum of the cumulative time taken for the entirety of the route shown in Figure 6c, for example). \square

Based on exactly the same reasoning as in the previous section, the continuous approximation

of problem (10) is given by

$$\underset{\mathcal{L} \in \text{Loop}(\mathcal{R})}{\text{minimize}} \frac{1}{\phi_0} \text{length}(\mathcal{L}) + \frac{2n}{\phi_1} \iint_{\mathcal{R}} f(x) d(x, \mathcal{L}) dx \quad (11)$$

and is similarly describable in terms of asymptotic analysis:

Theorem 12. *For fixed \mathcal{R} , f , ϕ_0 , and ϕ_1 , the optimal objective value $\text{OPT}(n)$ to problem (11) satisfies*

$$\text{OPT}(n) \sim \sqrt{\frac{2n}{\phi_0 \phi_1}} \cdot \iint_{\mathcal{R}} \sqrt{f(x)} dx$$

as $n \rightarrow \infty$.

Proof. This is the exact same reasoning as Theorem 10 and we omit it for brevity. \square

3.3 Remarks and variations

We have now derived upper and lower bounds of a continuous relaxation of (1) that are proportional to $\sqrt{\frac{n}{\phi_0 \phi_1}} \cdot \iint_{\mathcal{R}} \sqrt{f(x)} dx$, and that differ from one another by a factor of 2. Thus, we adopt the expression

$$\text{Time to perform service} \approx \beta' \sqrt{\frac{n}{\phi_0 \phi_1}} \cdot \iint_{\mathcal{R}} \sqrt{f(x)} dx$$

where β' is some constant satisfying $1/\sqrt{2} \leq \beta' \leq \sqrt{2}$. In addition, by Theorem 2, we see that the amount of time needed to visit n customers sampled from f using *only* a truck (and no UAVs) is asymptotically equal to $\beta \frac{\sqrt{n}}{\phi_0} \cdot \iint_{\mathcal{R}} \sqrt{f(x)} dx$, and it is estimated that $\beta \approx 0.7124$ [6]. Hence, the percent improvement that is gained by augmenting a truck with a UAV can be approximated as

$$\frac{\text{Service time without UAVs}}{\text{Service time with UAVs}} \approx \frac{\beta \frac{\sqrt{n}}{\phi_0} \cdot \iint_{\mathcal{R}} \sqrt{f(x)} dx}{\beta' \sqrt{\frac{n}{\phi_0 \phi_1}} \cdot \iint_{\mathcal{R}} \sqrt{f(x)} dx} = \alpha \sqrt{\frac{\phi_1}{\phi_0}}, \quad (12)$$

where $\alpha = \beta/\beta'$ lies between 0.5037 and 1.0075 (based on the estimate that that $\beta \approx 0.7124$ and the fact that $1/\sqrt{2} \leq \beta' \leq \sqrt{2}$). Thus, we hypothesize that the gains in efficiency due to introducing a UAV are proportional to $\sqrt{\phi_1/\phi_0}$, and we will estimate α in Section 4 (which would obviously also give us an estimate for β').

Non-Euclidean distances It is important to recognize that, while UAV trajectories are always measured in a Euclidean sense, the truck paths are not (since they are constrained by a road network). One way to compensate for a heterogeneous road network is by computing an “adjusted speed” ϕ_0 for the truck as follows: initially, given the n locations of our customers, we compute a TSP tour of those locations (using the road network) and report the length ℓ_0 of that tour (with respect to the road network) and the amount of time t_0 needed to visit those locations. An obvious estimate for ϕ_0 would then be to take ℓ_0/t_0 . A better “adjusted” estimate is obtained by defining ℓ'_0 to be the *Euclidean* length of the tour of the n points when visited in the same sequence as in the TSP tour on the road network, and estimating $\phi_0 = \ell'_0/t_0$. This results in smaller values of ϕ_0 because $\ell'_0 \leq \ell_0$. In other words, we treat the truck as if it is travelling in a Euclidean sense, but at a sufficiently slow speed that the amount of time to travel from one point to the next is the same as if the truck had been using a road network.

4 Computational results

In this section we conduct two computational experiments. The first experiment is done in the unit square with uniformly distributed demand, which we use to estimate the coefficient α introduced in equations (12) and (??). The second experiment uses these estimates of α to make predictions about the improvements in efficiency when demand follows a non-uniform distribution and real-time driving information on a road network is used.

4.1 Experiments using Euclidean distances

In our first experiment, we sample $n = 500$ points uniformly in the unit square, we fix a truck speed of $\phi_0 = 1$, and we allow the UAV speed ϕ_1 to vary with $\phi_1 \in \{1.5, 2, 3, 5\}$. The number of UAVs, k , also varies with $k \in \{1, 2, 3, 5\}$. Because of the difficulty of solving a given problem instance to optimality, we apply the following intuitive heuristic rule:

- Stage 1:
 - Assume initially that points p_1, \dots, p_n are ordered according to their optimal TSP tour.
 - The targets of the k UAVs are initially set to the points p_1, \dots, p_k .

- The truck always drives towards the next point that is not currently a target of any of the UAVs (for example, initially, the truck drives towards p_{k+1}).
 - Each UAV flies to its target and returns to the truck, at which point its new target becomes the next point that is not currently a target of any of the UAVs.
- Stage 2:
 - After recording the sequence of events that occurred in Stage 1, we have a list of the points that each UAV visited, which is written as P^i , for $i \in \{1, \dots, k\}$.
 - Solve the following convex optimization problem, which finds an optimal horsefly tour for fixed ordered assignments P^i :

$$\begin{aligned}
 & \underset{x_1, \dots, x_{n+1}, t_1, \dots, t_{n+1}}{\text{minimize}} \quad t_{n+1} \quad \text{s.t.} \\
 & t_r \geq t_q + (\|x_q - p_q\| + \|p_q - x_r\|)/\phi_1 \quad \forall (q, r) : q = P_j^i, r = P_{j-1}^i \\
 & t_i \geq t_{i-1} + \|x_i - x_{i-1}\|/\phi_0 \quad \forall i \in \{2, \dots, n+1\} \\
 & t_1 = 0 \\
 & x_1 = x_{n+1}.
 \end{aligned}$$

Figure 7 shows two of the solutions that are obtained when using this procedure. Table 1 shows the estimates of the coefficient α as computed by performing the above procedure 50 times for each pair of ϕ_1 and k (hence, $50 \times 4 \times 4$ trials in total). Each estimate $\hat{\alpha}$ is obtained by computing the TSP tour of the sampled points p_1, \dots, p_{500} as well as the horsefly tour that results from performing the heuristic above, and then setting

$$\hat{\alpha} = \frac{\text{Service time without UAVs}}{\text{Service time with UAVs} \cdot \sqrt{k\phi_1/\phi_0}}; \quad (13)$$

the values shown in the table are simply the averages of the 50 different trials. Note that, for fixed k , the estimates of α are more or less consistent for varying ϕ_1 , and that α seems to decrease in terms of k . The results shown are for the most part consistent with our prediction that $0.3562 \leq \alpha \leq 1.0075$. Thus, by taking averages over the columns of Table 1, we estimate that for $k = 1$, we have $\alpha = 1.00$, for $k = 2$, we have $\alpha = 0.91$, for $k = 3$, we have $\alpha = 0.84$, and for $k = 5$, we have $\alpha = 0.78$.

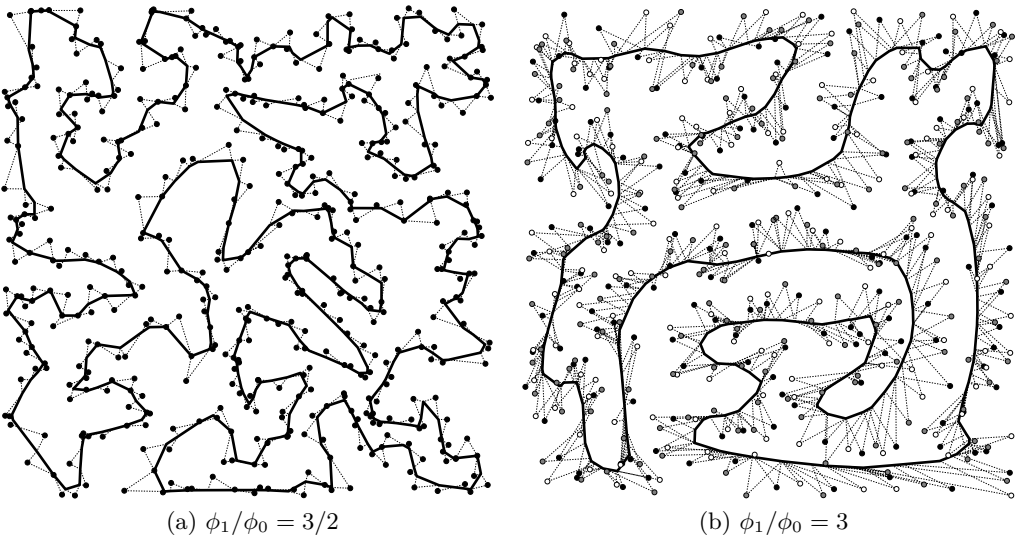


Figure 7: Two different horsefly tours with $k = 1$ and $\phi_1 = 1.5$ (a) and with $k = 3$ and $\phi_1 = 3$ (b); in the latter, the different colors of the points p_i (black, gray, and white) indicate which of the three UAVs visits that point.

		k			
		1	2	3	5
ϕ_1	1.5	1.02	0.88	0.84	0.80
	2	1.00	0.93	0.86	0.78
	3	0.95	0.89	0.85	0.74
	5	1.02	0.92	0.83	0.80

Table 1: Estimates of α , the proportionality term introduced in equations (12) and (??).

4.2 Experiments using road network distances

In our second experiment, we use the results of the preceding section to predict the changes in service time when UAVs are introduced to a truck that visits a collection of n destination points in a map of Pasadena, California, with $n \in \{25, 50, 100\}$. These n destination points are sampled uniformly from the centers of all 1734 US census blocks that belong to Pasadena, as shown in Figure 8b, which were obtained from [1]. Next, we compute a TSP tour of those n points with respect to the road network distance, as shown in Figure 8c; the length and duration of this TSP tour is estimated using the Google Maps Directions API [3], the Google Distance Matrix API [17], and the Concorde TSP Solver [2]. Finally, we apply the same two-stage heuristic from the previous section to compute a horsefly tour of those same points, as shown in Figure 8d. The “adjusted” truck speed ϕ_0 is generally around $20 \frac{\text{km}}{\text{hr}}$ in these experiments, and the UAV speed ϕ_1 satisfies $\phi_1 \in \{30 \frac{\text{km}}{\text{hr}}, 40 \frac{\text{km}}{\text{hr}}, 50 \frac{\text{km}}{\text{hr}}, 60 \frac{\text{km}}{\text{hr}}\}$.

Based on our preceding analysis (namely, equations (??) and (13)), we expect that the two service times should satisfy

$$\text{Service time with UAVs} = \frac{\text{Service time without UAVs}}{\alpha \cdot \sqrt{k\phi_1/\phi_0}}, \quad (14)$$

where there is $k = 1$ UAV and so we use $\alpha = 1.00$ (as determined from the previous section). Figure 9 shows these “predicted” service times compared with the actual service times for 10 individual experiments for $n \in \{25, 50, 100\}$ and $\phi_1 \in \{30 \frac{\text{km}}{\text{hr}}, 40 \frac{\text{km}}{\text{hr}}, 50 \frac{\text{km}}{\text{hr}}, 60 \frac{\text{km}}{\text{hr}}\}$. The “quality” of our approximation, so to speak, is therefore obtained by dividing the actual time by the predicted times (which we hope is close to 1); Figure 10 shows a histogram of these ratios, which confirms that our approximation is indeed a sensible “back-of-the-envelope” estimate of the true service time. Figures 11 and 12 show essentially the same thing for a set of experiments in which we fix $n = 100$ instead and we allow k to vary with $k \in \{2, 3, 5\}$, where we again see that the predictions are faithful to the true service times.

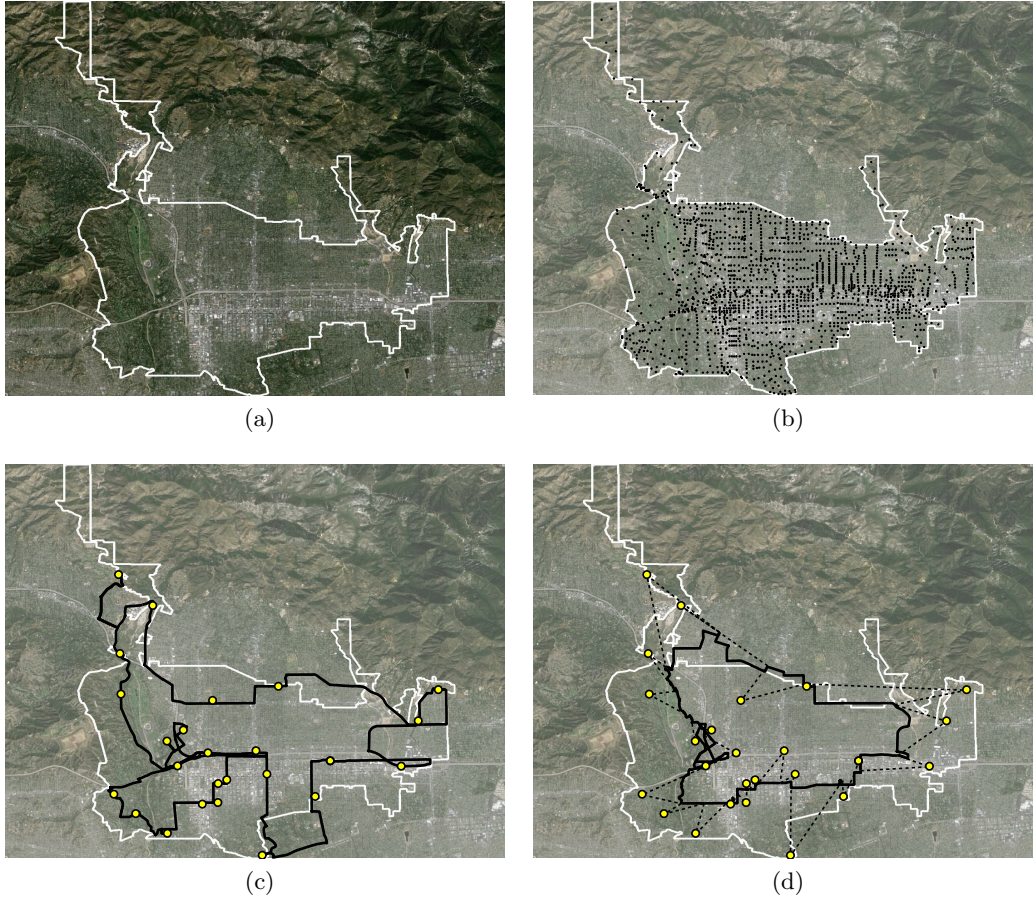
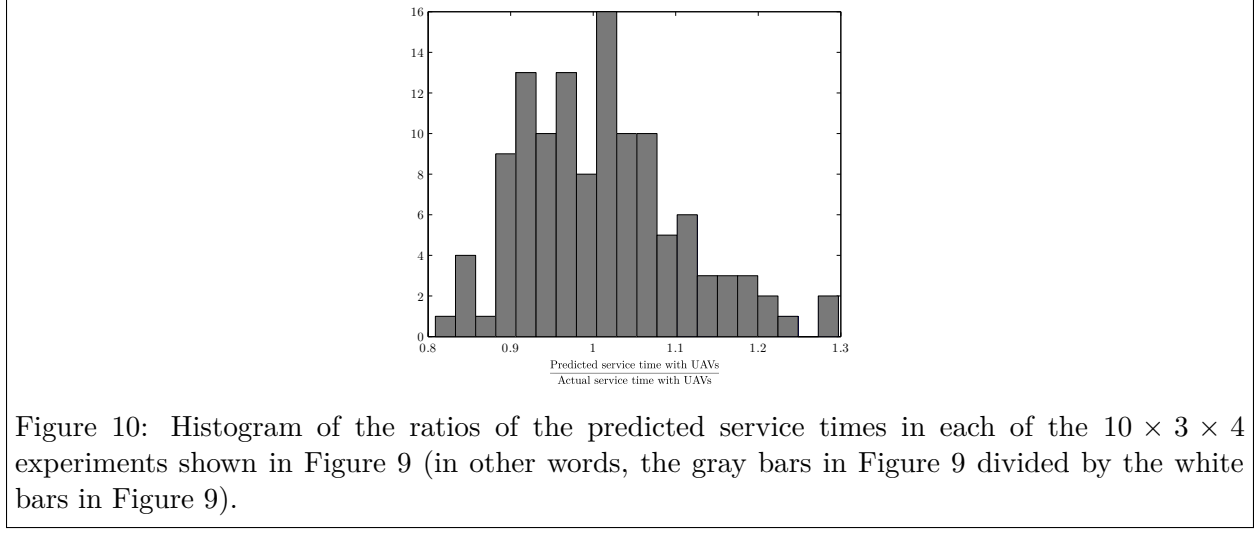
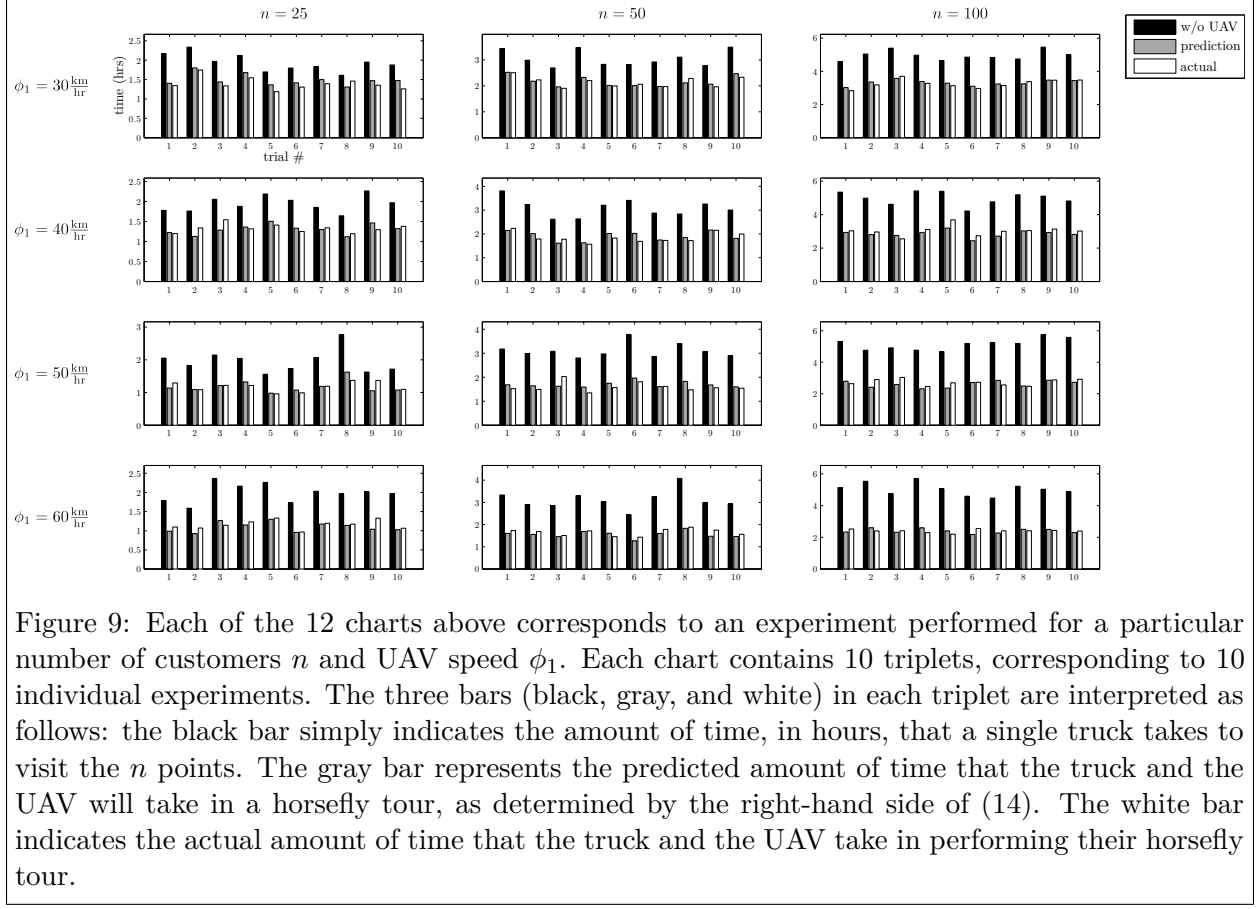


Figure 8: Figure (a) shows a map of Pasadena, California, and (b) shows the initial dataset consisting of the centers of all 1734 US census blocks located in Pasadena, California. Figure (c) shows the TSP tour with respect to the road network of $n = 25$ points sampled from those centers, and (d) shows the horsefly tour computed using the two-stage heuristic from Section 4.1.



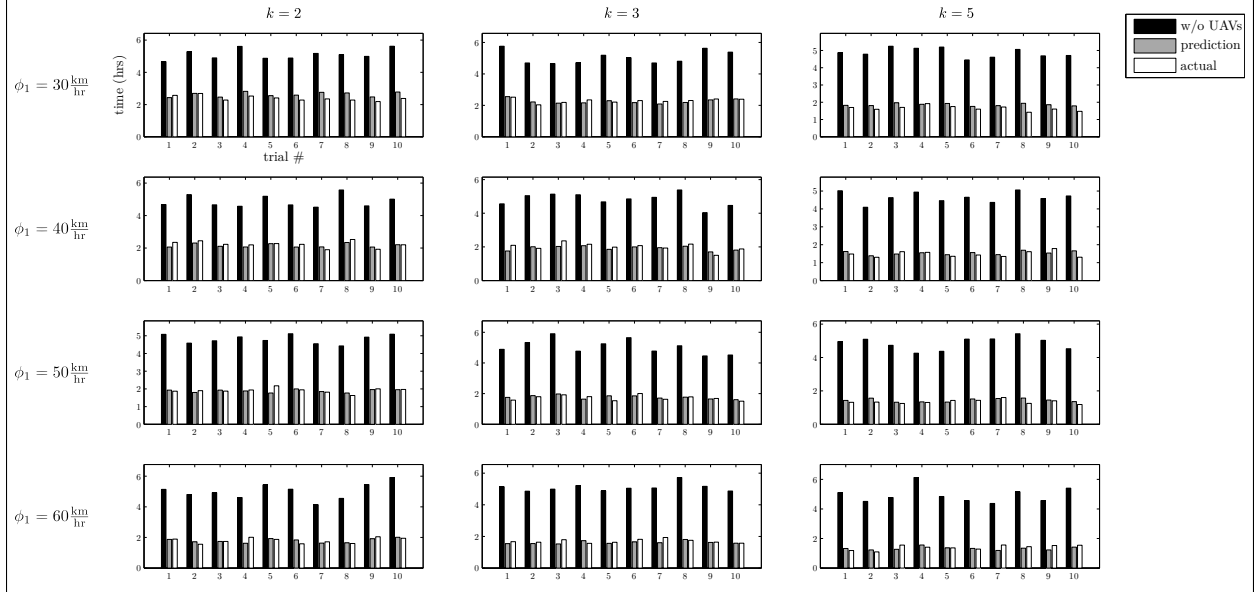


Figure 11: Each of the 12 charts above corresponds to an experiment performed for a particular number of UAVs k and UAV speed ϕ_1 ; the interpretation of these is the same as that of Figure 9.

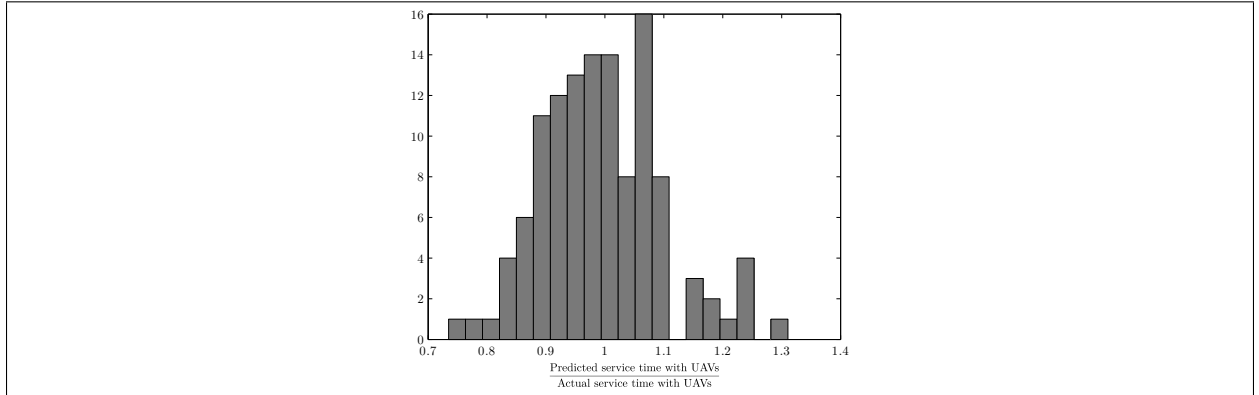


Figure 12: Histogram of the ratios of the predicted service times in each of the $10 \times 3 \times 4$ experiments shown in Figure 11 (in other words, the gray bars in Figure 11 divided by the white bars in Figure 11).

5 Conclusions

By using an asymptotic theoretical analysis in the Euclidean plane as well as a collection of computational experiments, we have concluded that the improvement in efficiency due to augmenting a delivery truck with a UAV is proportional to the square root of the ratio of the speeds of the truck and the UAV. One of the weak points in our analysis is the fact that we use heuristic methods to compute the coordinated routes between the truck and the UAV, rather than a true globally optimal solution. While we are unaware at present of any techniques that find these solutions for the problem scales discussed in this paper, we expect them to become available in the coming years as interest in UAVs in logistics increases.

References

- [1] 2010 Census Block Maps - Geography - U.S. Census Bureau. <https://www.census.gov/geo/maps-data/maps/block/2010/>. [Online; accessed 22-August-2015].
- [2] Concorde TSP Solver. <http://www.math.uwaterloo.ca/tsp/concorde.html>. [Online; accessed 22-October-2015].
- [3] Google Maps Directions API. <https://developers.google.com/maps/documentation/directions/>. [Online; accessed 22-October-2015].
- [4] U.S. Forest Service UAS policy. <http://www.fs.fed.us/science-technology/fire/unmanned-aircraft-systems>.
- [5] N. Agatz, P. Bouman, and M. Schmidt. Optimization approaches for the traveling salesman problem with drone. *ERIM Report Series Reference No. ERS-2015-011-LIS*, 2015.
- [6] D. Applegate, W. Cook, D. S. Johnson, and N. J. A. Sloane. Using large-scale computation to estimate the Beardwood-Halton-Hammersley TSP constant. Presentation at 42 SBPO, 2010.
- [7] J. Beardwood, J. H. Halton, and J. M. Hammersley. The shortest path through many points. *Mathematical Proceedings of the Cambridge Philosophical Society*, 55(4):299–327, 1959.

- [8] G. Bensinger. Amazon's drones for deliveries. *Wall Street Journal*, Dec 2013. <http://blogs.wsj.com/digits/2013/12/01/amazons-bezos-shows-flying-drones-for-package-delivery/>.
- [9] V. Bryan. Drone delivery: DHL 'parcelcopter' flies to German isle. *Reuters*, Sep 2014. <http://www.reuters.com/article/2014/09/24/us-deutsche-post-drones-idUSKCN0HJ1ED20140924>.
- [10] L. D. Burns, R. W. Hall, D. E. Blumenfeld, and C. F. Daganzo. Distribution strategies that minimize transportation and inventory costs. *Operations Research*, 33(3):469–490, 1985.
- [11] G. P. Cachon. Retail store density and the cost of greenhouse gas emissions. *Management Science*, 60(8):1907–1925, 2014.
- [12] J. F. Campbell, A. T. Ernst, and M. Krishnamoorthy. Hub arc location problems: part I – introduction and results. *Management Science*, 51(10):1540–1555, 2005.
- [13] J. F. Campbell and M. E. O’Kelly. Twenty-five years of hub location research. *Transportation Science*, 46(2):153–169, 2012.
- [14] V. Culpan. Watch how Swiss Post is delivering with drones. *Wired*, Jul 2015. <http://www.wired.co.uk/news/archive/2015-07/09/swiss-delivery-drones>.
- [15] C. Daganzo. *Logistics Systems Analysis*. Springer, 2005.
- [16] R. D’Andrea. Guest editorial: Can drones deliver? *Automation Science and Engineering, IEEE Transactions on*, 11(3):647–648, 2014.
- [17] Google Developers. The Google Distance Matrix API. <https://developers.google.com/maps/documentation/distancematrix/intro>, 2015.
- [18] L. Evers, T. Dollevoet, A. I. Barros, and H. Monsuur. Robust UAV mission planning. *Annals of Operations Research*, 222(1):293–315, 2014.
- [19] L. Few. The shortest path and the shortest road through n points. *Mathematika*, 2:141–144, 1955.

- [20] M. Gendreau, A. Hertz, and G. Laporte. A tabu search heuristic for the vehicle routing problem. *Management Science*, 40(10):1276–1290, 1994.
- [21] M. Gendreau, G. Laporte, C. Musaraganyi, and É. D. Taillard. A tabu search heuristic for the heterogeneous fleet vehicle routing problem. *Computers & Operations Research*, 26(12):1153–1173, 1999.
- [22] Q. M. Ha, Y. Deville, Q. D. Pham, and M. H. Hà. On the min-cost traveling salesman problem with drone. *arXiv preprint arXiv:1512.01503*, 2015.
- [23] M. Haimovich and Thomas L. Magnanti. Extremum properties of hexagonal partitioning and the uniform distribution in Euclidean location. *SIAM J. Discrete Math.*, 1:50–64, 1988.
- [24] B. Hajek. *Random Processes for Engineers*. Cambridge University Press, 2015.
- [25] M. Heutger and M. Kückelhaus. Unmanned aerial vehicle in logistics: a DHL perspective on implications and use cases for the logistics industry. Technical report, DHL Trend Research, 2014. http://www.dhl.com/content/dam/downloads/g0/about_us/logistics_insights/DHL_TrendReport_UAV.pdf.
- [26] D. S. Hochbaum. When are NP-hard location problems easy? *Annals of Operations Research*, 1:201–214, 1984.
- [27] M. Huang, K. R. Smilowitz, and B. Balcik. A continuous approximation approach for assessment routing in disaster relief. *Transportation Research Part B: Methodological*, 50:20–41, 2013.
- [28] O. Jabali, M. Gendreau, and G. Laporte. A continuous approximation model for the fleet composition problem. *Transportation Research Part B: Methodological*, 46(10):1591–1606, 2012.
- [29] M. Kanellos. Google working on drones too. *Forbes*, Aug 2014. <http://www.forbes.com/sites/michaelkanellos/2014/08/29/google-working-on-drones-too/>.
- [30] S.G. Krantz and H.R. Parks. *Geometric Integration Theory*. Cornerstones Series. Birkhäuser, 2008.

- [31] M. Kress and J. O. Royset. Aerial search optimization model (ASOM) for UAVs in special operations. *Military Operations Research*, 13(1):23–33, 2008.
- [32] C. K. Y. Lin. A vehicle routing problem with pickup and delivery time windows, and coordination of transportable resources. *Computers & Operations Research*, 38(11):1596–1609, 2011.
- [33] A. Madrigal. Inside the drone missions to Fukushima. *The Atlantic*, Apr 2011. <http://www.theatlantic.com/technology/archive/2011/04/inside-the-drone-missions-to-fukushima/237981/>.
- [34] C. McCall. Sea Shepherd says drones find, photograph Japan’s whaling fleet. *Reuters*, Dec 2011. <http://www.reuters.com/article/2011/12/25/us-australia-japan-whaling-idUSTRE7B001K20111225>.
- [35] C. C. Murray and A. G. Chu. The flying sidekick traveling salesman problem: Optimization of drone-assisted parcel delivery. *Transportation Research Part C: Emerging Technologies*, 54:86–109, 2015.
- [36] C. H. Papadimitriou. Worst-case and probabilistic analysis of a geometric location problem. *SIAM Journal on Computing*, 10:542, 1981.
- [37] C. Redmond and J. E. Yukich. Limit theorems and rates of convergence for euclidean functionals. *The Annals of Applied Probability*, 4(4):pp. 1057–1073, 1994.
- [38] R. Smith. Utilities turn to drones to inspect power lines and pipelines. *Wall Street Journal*, May 2015. <http://www.wsj.com/articles/utilities-turn-to-drones-to-inspect-power-lines-and-pipelines-1430881491>.
- [39] J. M. Steele. Subadditive Euclidean functionals and nonlinear growth in geometric probability. *The Annals of Probability*, 9(3):pp. 365–376, 1981.
- [40] J.M. Steele. *Probability Theory and Combinatorial Optimization*. CBMS-NSF Regional Conference Series in Applied Mathematics. Society for Industrial and Applied Mathematics, 1987.

- [41] P. Toth and D. Vigo. *The vehicle routing problem*. Society for Industrial and Applied Mathematics, 2001.
- [42] X. Wang, S. Poikonen, and B. Golden. The vehicle routing problem with drones: several worst-case results. *Optimization Letters*, pages 1–19, 2016.
- [43] M. Wohlsen. The next big thing you missed: Amazon’s delivery drones could work – they just need trucks. *Wired*, Jun 2014. <http://www.wired.com/2014/06/the-next-big-thing-you-missed-delivery-drones-launched-from-trucks-are-the-future-of-ship>
- [44] E. Wygonik and A. Goodchild. Evaluating the efficacy of shared-use vehicles for reducing greenhouse gas emissions: a US case study of grocery delivery. In *Journal of the Transportation Research Forum*, volume 51, 2012.
- [45] W. Xie and Y. Ouyang. Optimal layout of transshipment facility locations on an infinite homogeneous plane. *Transportation Research Part B: Methodological*, 75:74–88, 2015.

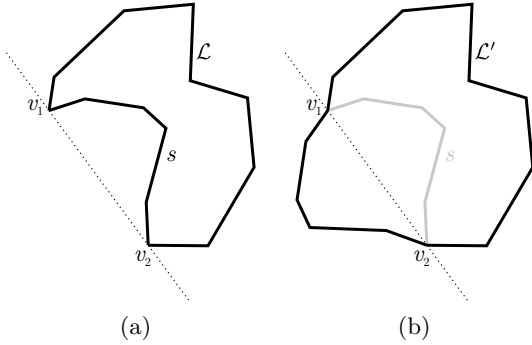


Figure 13: Reflecting the polygonal chain s about the line joining v_1 and v_2 .

Appendix: Proof of Lemma 3

The assumption that \mathcal{L} is polygonal is a valid one because the standard definition of the length of \mathcal{L} is simply the limit of a discretization; if we say that \mathcal{L} is the image of the continuous mapping $\gamma : [0, 1] \rightarrow \mathbb{R}^2$, then the length of \mathcal{L} is defined as

$$\text{length}(\mathcal{L}) = \sup_{0=t_0 < t_1 < \dots < t_M=1} \sum_{i=1}^{M-1} \|\gamma(t_i) - \gamma(t_{i-1})\|$$

where the supremum is taken over all possible partitions of $[0, 1]$ and M is unbounded.

The assumption that \mathcal{L} forms the boundary of a convex region is also straightforward: at the very least, we can certainly assume that \mathcal{L} is *simple*, that is, that \mathcal{L} does not intersect itself (since one can always “un-cross” a pair of intersecting edges of \mathcal{L} in an obvious way). If \mathcal{L} is not the boundary of a convex region, then (since we have assumed that \mathcal{L} is polygonal) there must exist a pair of vertices v_1, v_2 of \mathcal{L} such that v_1 and v_2 are adjacent on the convex hull $\text{Conv}(\mathcal{L})$ of \mathcal{L} , but *not* adjacent on \mathcal{L} itself; see Figure 13a. If we let s denote the component of \mathcal{L} that lies between v_1 and v_2 , then it is obvious that we can reflect s about the line joining v_1 and v_2 , to obtain a new curve \mathcal{L}' with the same length as \mathcal{L} , as shown in Figure 13b. It is then an entirely straightforward argument to verify that, for any ϵ , we have $\text{Area}(N_\epsilon(\mathcal{L}')) \geq \text{Area}(N_\epsilon(\mathcal{L}))$, which completes the proof.